# Fast Characterization of Power LEDs: Circuit Design and Experimental Results

Nicola Roccato, *Graduate Student Member, IEEE*, Francesco Piva, *Associate Member, IEEE*, Matteo Buffolo, *Member, IEEE*, Nicola Trivellin, Carlo De Santi, *Member, IEEE*, Claudio Narduzzi, *Life Member, IEEE*, Riccardo Fraccaroli, Alessandro Caria, Gaudenzio Meneghesso, *Fellow, IEEE*, Enrico Zanoni, *Life Fellow, IEEE*, and Matteo Meneghini, *Senior Member, IEEE*

***Abstract*— A precise measurement of optical power, forward voltage, and junction temperature of light-emitting diodes (LEDs) is the key for characterization and health monitoring of these devices. In many cases, LED characterization is carried out with relatively long (10 ms and longer) pulses, that is, in conditions in which self-heating can significantly impact measurement results. To overcome this limitation, this article proposes a fast and versatile measurement approach based on a specifically designed current source, with a maximum current of about 1 A, high stability (variations under 0.1%) and settling time <20 $\mu$s, and demonstrates its applicability to pulsed and transient characterization of power LEDs. The proposed system has the inherent advantages of 1) permitting a fast pulsed characterization of the devices, which—as we demonstrate—is much more accurate than quasipulsed or dc analysis; 2) allowing isothermal characterization of LEDs without requiring long settling times, with beneficial impact on the throughput of LED characterization; 3) allowing characterization of the voltage heating transient (during constant current operation), which is the key for junction temperature and thermal resistance extraction, as well as for the development of compact models; 4) monitoring the optical power during the self-heating transient; and 5) the spectrum of the device providing additional information, such as the peak-shift or the phosphor behavior. The efficacy of the proposed approach has been demonstrated by testing commercial LEDs: the results clearly indicate that a fast (<20 $\mu$s) LED characterization is necessary for a proper extraction of the main spectral parameters and of the related temperature dependence.**

***Index Terms*— Electro-optical characterization, light-Emitting diodes (LEDs), optoelectronic devices, photothermal effects, self-heating, temperature measurement, thermal analysis.**

Manuscript received 24 November 2023; revised 7 February 2024, 13 March 2024, and 17 April 2024; accepted 19 April 2024. Date of publication 8 May 2024; date of current version 23 May 2024. This work was supported by the Electronics Components and Systems for European Leadership Joint Undertaking (ECSEL-JU) under Grant 101007319. The JU receives support from the European Union's Horizon 2020 research and innovation programme and Netherlands, Hungary, France, Poland, Austria, Germany, Italy, Switzerland. The review of this article was arranged by Editor S.-M. Lee. *(Corresponding author: Nicola Roccato.)*

Nicola Roccato, Francesco Piva, Matteo Buffolo, Carlo De Santi, Claudio Narduzzi, Riccardo Fraccaroli, Alessandro Caria, Gaudenzio Meneghesso, and Enrico Zanoni are with the Department of Information Engineering, University of Padova, 35131 Padua, Italy (e-mail: roccatonic@dei.unipd.it).

Nicola Trivellin is with the Department of Information Engineering, and the Department of Industrial Engineering, University of Padova, 35131 Padua, Italy.

Matteo Meneghini is with the Department of Information Engineering, and the Department of Physics and Astronomy, University of Padova, 35131 Padua, Italy.

Color versions of one or more figures in this article are available at https://doi.org/10.1109/TED.2024.3393448.

Digital Object Identifier 10.1109/TED.2024.3393448

## I. Introduction

HIGH-POWER optoelectronic devices, such as laser diodes (LDs) and light-emitting diodes (LEDs), have a huge potential application market in different fields, such as high brightness illumination, streetlights, automotive, and full-color displays [1], [2], [3]. The latest advancements in the LED field led to steadily shrinking device packages and ever-increasing operating current densities, thus exacerbating self-heating effects. To ensure optimal efficiency and long lifetime of LEDs, efficient thermal management is thus critical, especially when these devices are employed in thermally constrained environments [4], [5].

A first important step in device characterization is the analysis of voltage and optical power self-heating transients after turn-on. This is typically done through the analysis of transients under constant current bias. In particular, voltage is used as a temperature-sensitive parameter (TSP) with proper calibration, and voltage transients can be directly converted into temperature transients, thus permitting the accurate extraction of junction temperature ($T_j$) and thermal resistance [6], [7]. Analyzing the self-heating transients is of fundamental importance for 1) extracting (from the behavior at $t = 0$) information on the LED performance when the junction is "cold" (i.e., before the self-heating transient), or at a specified $T_j$; 2) analyzing the variation in LED optical power induced by self-heating (it is well known that LEDs show a considerable output power drop when subjected to self-heating); and 3) extrapolating through analysis of voltage transients and related structure functions, the value of the thermal impedance. At the current state of art, the heating transient analysis are performed indirectly, by applying first a constant high current and subsequently measuring the voltage transient during device cooling, at lower current values [7], [8], [9], [10]. Thus, this

procedure does not keep into consideration the heating effects of the measuring current and does not allow the monitoring of the optical and spectral characteristics of the device during the self-heating phase.

In addition, a fast-current source is required also for electrooptical and spectral measurements, which must be carried out when LEDs are in the switched-ON state (CIE 127:2007). Measurements are typically performed as in-line tests (CIE 226:2017) or laboratory tests (CIE 225:2017), with measurement windows in the range of 10–100 ms (for in-line testing) or even at dc (for laboratory testing). These times are much longer than the heating transients of LEDs, making isothermal characterization a time-consuming task. A faster measurement methodology would substantially simplify LED characterization by enabling the execution of pulsed measurements during which the junction is at the same temperature as the environment/base plate (iso-thermal), instead of waiting for the execution of measurements in steady-state dc regime.

Despite the importance of fast and accurate measurement techniques for LED characterization, currently no commercial instrument is able to provide a complete characterization of the self-heating transients and fast spectral and electrooptical measurements. Some recent works [6], [11], [12], [13], [14] target to perform isothermal IVL characterizations, but adopt time-consuming procedures, often combining different dc measurements. Issues regarding the precision of the measurement and of the current source, as well as the capability to perform fast enough electrooptical characterization, limit the performance of these methodologies.

Therefore, the aim of this article is to propose a measurement methodology fully compatible with requirements for the pulsed (iso-thermal) and transient characterization of LEDs. This kind of analysis requires the design of a specific measurement setup equipped with an accurate current sources, capable of high current output (up to 1 A, for power LEDs), high temporal stability in order to record the temperature variations with high accuracy, and fast settling times (shorter than LED self-heating transients [15]). Thanks to the use of a feedback network based on an instrumentation amplifier and a subtractor, the circuit is intrinsically immune to supply voltage fluctuations and ensures temporal stability better than 0.1% over a long (more than 100 s) pulse generation interval. After circuit design, simulation, and implementation, circuit performance was evaluated in detail: tests carried out on commercial blue, white, and red high-power LEDs show the good quality of the measurement results essential for a deeper analysis of the LED characteristics and reliability. In particular, the developed setup is capable of performing a characterization of the heating transient directly, at the desired load current, and to also monitor the optical power transients and the spectral variations. For white LEDs, the latter provide useful information on phosphors behavior during early optical transient, which has not been reported so far. Finally, the setup also allows the extrapolation of the junction temperature trend, exploiting the relation between $T_j$ and the device voltage obtained by isothermal $T_j$-$V_f$ measurements. Additional data analysis can then be performed to derive the related structure function, and thermal resistance, of the device under test (DUT) [9], [16], [17].

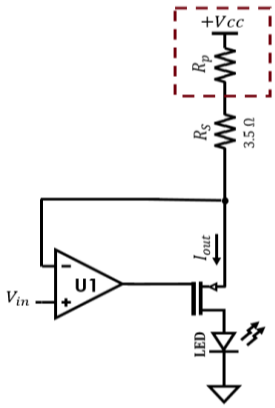


Fig. 1. Schematic representation of the voltage to current converter. This circuit has an intrinsic sensitivity to the instability in supply voltage, that is, addressed in the final implementation.

## II. Current Source Circuit

### A. Circuit Operation

The first step to carry out the LED characterization is the design of the specific current source. Recent reports [18], [19] proposed designs of precision current sources; however, these solutions are unsuitable for the high current levels required for power LEDs. Other recent articles focus on high-speed LED drivers working down to the nanosecond scale [20], [21], [22], [23], but their application remains limited to pulsed test of optoelectronic devices, without focusing on the long-term analysis of the heating transients.

Specifications of the circuit implemented in this work are 1) output current of up to 1 A; 2) settling time of about 10–20 $\mu s$; and 3) high current stability, with a steady-state fluctuation lower than 0.1%. To achieve this, we started by investigating the approaches proposed in [18] and [19] that deal with high-precision voltage-controlled current sources. We decided to base our circuit on the voltage to current converter (load branch) in Fig. 1. Here the output current flowing through the DUT is set by controlling voltage across the sensing resistor $R_S$. Neglecting parasitic resistance $R_P$, the voltage across $R_S$ is equal to $V_{PS} - V_{in}$, where $V_{PS}$ is the power supply voltage and $V_{in}$ is the input voltage at the noninverting input of operational amplifier U1. Therefore, in steady-state condition, the output current is defined as

$$I_{out} = \frac{V_{PS} - V_{in}}{R_S}. \tag{1}$$

In this circuit, $V_{PS}$ is set at 10 V, $R_S$ at 3.5 Ω, and consequently $V_{in}$ is set according to the target range for $I_{out}$.

By changing the sensing resistance value, it is possible to change the maximum set current and the current resolution of the circuit. With the configuration in Fig. 1, it is possible to achieve output currents ranging from 30 mA to about 1.3 A: the maximum output current is obtained when the sum of the LED, pMOS, and sensing resistance voltage is equal to 10 V, that is, the supply voltage of the load branch. For a lower maximum output current with higher setting resolution, it is

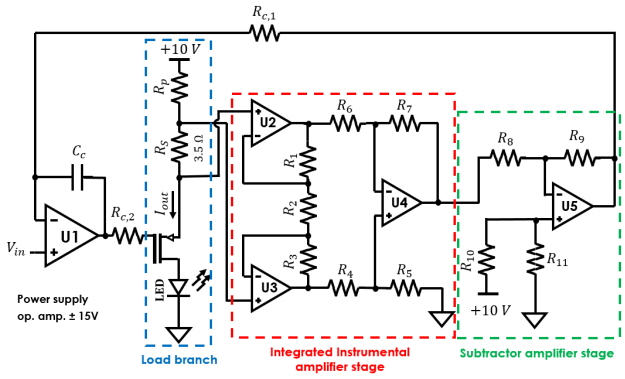


Fig. 2. Schematic representation of the circuit. The differential feedback allows to measure with variations under 0.1% the voltage across the sensing resistance.

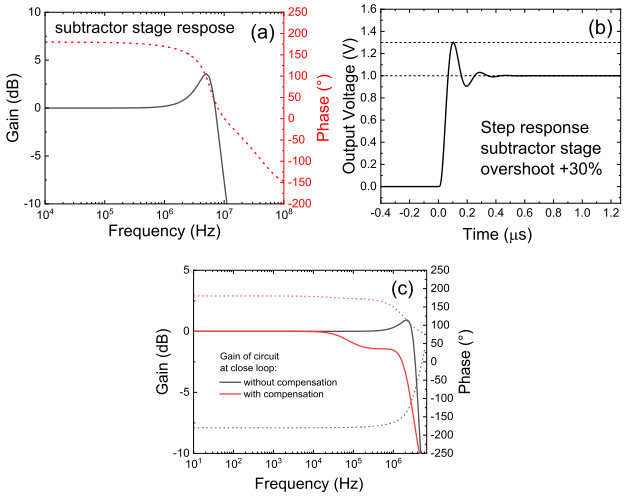


Fig. 3. (a) Bode diagram of the subtractor stage around 1 MHz. (b) Unitary step response of the subtractor. (c) Simulated frequency response of the circuit with and without the compensation net. The introduction of the single pole allows an attenuation at high frequencies.

sufficient to increase the sensing resistance value, or vice versa for the opposite case.

The simple voltage to current converter shown in Fig. 1 is not well suited for the purpose of this work. In fact, feedback for current control is based on the assumption that voltage on the upper terminal of $R_s$ is equal to the power supply voltage $V_{\mathrm{PS}}$. However, commercial power supply output voltage can present oscillations of about 1%. Besides the output resistance $R_P$ is not zero, and at the high current levels drawn by the circuit, it will have an impact on the voltage across $R_S$, and thus on the output current $I_{\mathrm{out}}$. For this reason, we opted to include differential sensing, and a related feedback loop, in order to control voltage across $R_S$.

To this aim, an instrumentation amplifier with unity gain was added to the circuit to measure the voltage $V_{Rs}$ across the sensing resistor $R_S$ (see red dashed line in Fig. 2). We note here that this stage alone is not sufficient to complete the feedback loop. In fact, the positive input voltage applied to the noninverting input of U1 is $10\mathrm{V} - V_{Rs}$, whereas the voltage at the output of the instrumentation amplifier is equal to $V_{Rs}$. Therefore, a subtractor stage, whose role is to subtract the measured $V_{Rs}$ from 10 V, was added in cascade to the instrumentation amplifier (see green dashed line in Fig. 2). The output of the subtractor is then fed to the inverting input of the operational amplifier U1 to achieve an accurate control of the output current $I_{\mathrm{out}}$.

We note that the adopted operational amplifier (the same typology has been used for U1 and U5) has a compensated frequency response: at unity gain, the magnitude of the gain is flat till 1 MHz, has an overshoot above 1 MHz, and a gain roll-off by >40 dB/dec above 20 MHz. When the operational amplifier is used in the subtractor, with unity gain, the Bode diagram of the magnitude of the gain shows a 3.5 dB overshoot around 5 MHz [see Fig. 3(a)]. This leads to an underdamped behavior that gives a 30% overshoot of step response of the subtractor [see Fig. 3(b)]. This results in an overshoot of the step response of the full circuit. To overcome this issue, a single-pole compensation network (composed of $R_{c,2}, C_c$) was added to the circuit (see Fig. 2), in order to smoothen the response and avoid current spikes and instabilities that may be detrimental to the DUT. The choice of the optimal values has been done through analysis of the frequency response of the components, which were carried out through the study of the datasheets and simulation analysis. We used LTspice with the correct model of the op-amps and of the MOSFET adopted in the circuit. Fig. 3(c) reports the frequency response of the whole circuit before and after the compensation. As can be noticed, the adopted compensation network effectively eliminates the overshoot in the frequency response. Besides the choice of the compensation values has been rather conservative to obtained a damped response and avoid current overshoot that could affect the following analysis.

## B. Circuit Implementation

For our testing purposes, the input voltage of the circuit can be driven by an arbitrary waveform generator (AWG), whereas the ± 15 V supply voltage for the amplifiers and the 10 V supply for the load were provided by laboratory-grade power supplies.

The specific choice of components was driven by the functional requirements of the circuit. In particular, the operational amplifiers need a high slew rate, over 200 V/$\mu$s to ensure fast circuit response, whereas the pMOS has to reach high current levels without significant self-heating. The operational amplifier chosen for U1 has a slew rate of 400 V/$\mu$s and a fast settling time of 230 ns for a 10 V step in addition to an output swing of ± 13 V under high load conditions. A further critical aspect is the self-heating of the sensing resistor during operation that may generate an unwanted variation of the output current. To overcome this issue, the sensing resistor was engineered as the parallel between three 10 W resistors, each with a value of 10 Ω. Our tests, carried out by imposing a 1 A constant current to the developed resistor network, and measuring the corresponding voltage, indicate a high stability of the resistance value (variations under the 1‰) over several hours (graph not shown for brevity).

We initially simulated the circuit in LTspice and then implemented it on PCB. In Fig. 4, we report a comparison between the voltage and current output of the circuit obtained

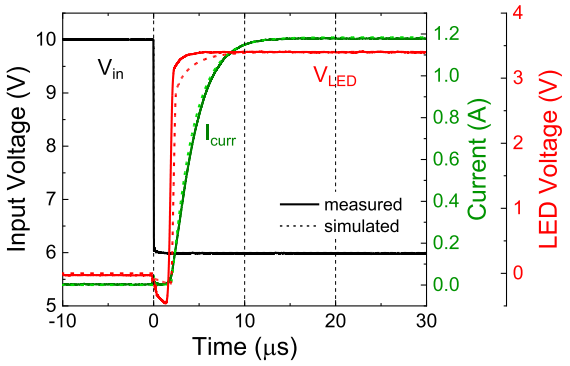


Fig. 4. Comparison of the transient response of the voltage and current between the simulated circuit by LTspice (dashed line) and the implemented circuit on PCB (measured line).

through simulations and by measurements on the implemented circuit: a great similarity with the expected results can be observed. Once the falling edge of the input voltage pulse (black line) gives the start to the current source, the current and voltage signals of a 630 nm LED are measured. The slight delay of the voltage and current turn-on with respect to the falling edge of the input pulse is due to the charge of the compensation capacitor $C_c$ and depends on the amplitude of the input pulse. This delay does not represent an issue, since for pulsed and transient measurements, the signal recording is synchronized with the rise of the LED voltage through a proper triggering sequence.

It can be observed that the output current (∼1.2 A) reaches its steady-state value in about 15 $\mu$s: the overall speed of the circuit depends on the integrated components adopted and on the compensation network. In particular, the integrated instrumentation amplifier included in the circuit exhibits a slow slew rate that decreases the settling time. Another possible solution is to implement this stage with discrete components, featuring faster operational amplifiers, or to reduce the settling time by modifying the compensation network but allowing the presence of a slight overshoot in the transient response.

## III. Sensitivity of the Circuit

### A. Optimization of Line Regulation

As mentioned in Section II, the output current has a strong dependence on the voltage across the sensing resistor. To ensure a high precision of the voltage across this resistor, we implemented the feedback circuit based on differential sensing, constituted by the instrumentation amplifier and by the subtractor. The stability of the steady-state output current as a function of the power supply voltage (line regulation) with and without this differential sensing is reported in Fig. 5.

As can be noticed, in the circuit without the differential feedback, the voltage variation of the power supply results in a significative deviation of the actual output current from the targeted one (about 7% versus a variation of 2% in the power supply voltage). By adopting the differential sensing solution, we were able to compensate this issue, making the output current independent of variations of the power supply voltage. These results confirm the effectiveness of the adopted approach.

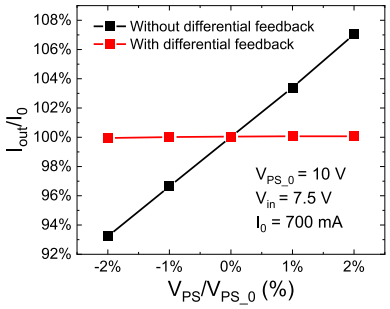


Fig. 5. Variation in the steady-state output current as a function of the deviation of power supply voltage, with and without the differential feedback configuration implemented in this article. The data have been measured after implementing both circuit topologies.

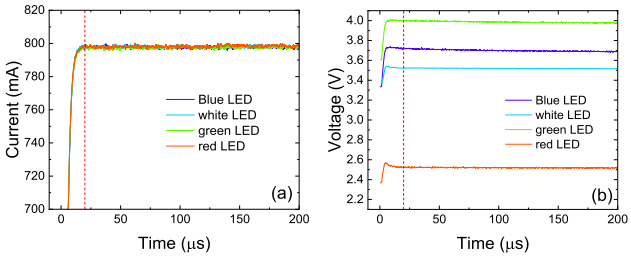


Fig. 6. Analysis of the load sensitivity of the circuit. The impedance of the load is varied by changing high-power LED. (a) Current waveform remains unchanged. (b) Load voltage scales with the LED under test.

### B. Sensitivity to Load

Sensitivity to the load impedance was also evaluated. To this aim, we tested the circuit with four different high-power LEDs (blue, white, green, and red) as load bias at 800 mA. In Fig. 6, we can observe that the load voltage scales as expected are with varying LED typology [Fig. 6(b)], whereas the current waveform remains constant [Fig. 6(a)], indicating the good performance of the circuit.

## IV. Analysis of Transients

The first main goal of the circuit proposed in this work is to allow the measurement of self-heating transients of optoelectronics devices. The measurement is based on the analysis of the voltage transients generated by a step in the LED current [17], [24], [25]. Assuming a 1-D heat flow, device self-heating leads to a decrease in the operating voltage, with several time constants which are related to the individual thermal interfaces within the LED structure. From a voltage transient measurement, it is thus possible to extrapolate the cumulative thermal capacitance and resistance toward the heat source, as seen from a specific point of the structure [17], [26]. We note here that in the latest thermal testing standards JESD 51-5x from JEDEC [27], this thermal transient characterization is performed indirectly by considering cooling transients [28], [29], [30] (instead of the heating transient) due to the lack of suitable instrumentation to carry out reliable measurements of the heating transients. The methodology proposed in this article can overcome this limitation, thus allowing to evaluate LED heating transients. Besides we note here an additional advantage of the possibility to record the whole heating transients of the optical emission: this allows us

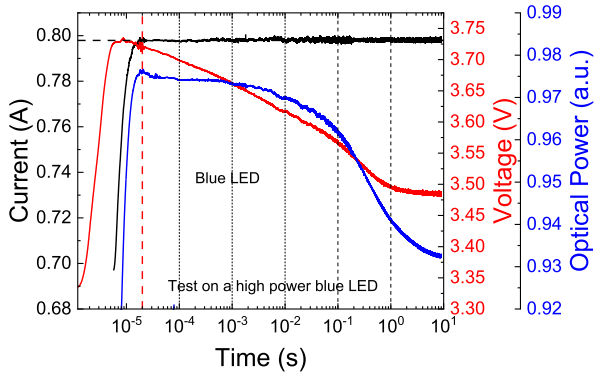


Fig. 7. Transient measurement of the current, voltage, and optical power on a blue LED biased at about 800 mA. It is possible to observe the decreasing trends of the voltage and optical power due to the self-heating of the device. The dot lines indicate the time positions of IVL measurements windows. Their width changes as a function of the sample rate adopted in the measurement interval.

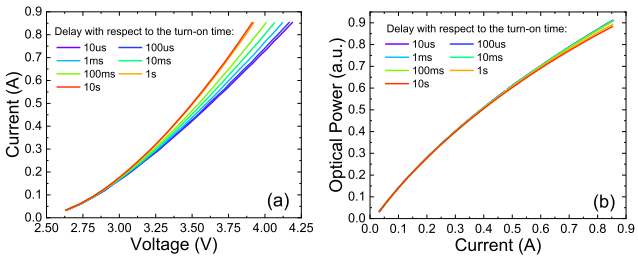


Fig. 8. (a) Current-voltage and (b) optical power-current characteristics as a function of the delay after the turn on of the LED.

to monitor the trend variation with also particular attention to the phosphors behavior and their heating in white LEDs [31]. All this information would not be available with the traditional characterization technique.

To test the implemented circuit, we analyzed a high-power 450 nm LED mounted on a heat sink. The measurement records the current, voltage, and optical power transients up to 10 s by means of a Tektronix MSO44 oscilloscope and a photodetector PDA10A-EC and results are graphed on a semilogarithmic scale. Three measurements have been executed with different time resolutions to measure a wide time-window, from the $\mu$s to the 10 s range after LED voltage turn on.

As shown in Fig. 7, the current reaches its steady-state value within 20 $\mu$s (red dashed line): we consider all the transients are completed after this time, that is, we consider that all voltage and OP measurements are carried out in a constant-current condition. We note here that—in such a wide time frame—the current exhibits a high stability, with fluctuations well below 1‰. The optical power and voltage transients (the blue and red curves, respectively) exhibit a decreasing trend, due to the device heating, and it is possible to distinguish different intervals, featuring different time constants, which are of fundamental importance for the creation of the thermal model. Considering that $T_j$ and the forward voltage of the device are directly linked [32], the data shows that the device starts to heat already after a few $\mu$s from the start as we can clearly observe in the graph looking at the voltage trend. In fact, the current, plotted with a high resolution around its steady-state value, reaches high levels before 20 $\mu$s, starting to heat the device and decreasing its voltage already from 6 $\mu$s after the turn-on. Finally, we note here that optical power is almost stable in the first 100 $\mu$s of operation: a pulsed characterization carried out in this time range can then provide a reliable iso-thermal reading of device properties.

## V. Pulsed I–V-L Measurements

By repeating the transient measurements described above at different current levels, one can obtain the current-voltage ($I-V$) and the optical power-current ($L-I$) characteristics as a function of the delay from the LED turn-on time. We refer to this as "turn-on time" the instant when the diode reaches its forward knee voltage (about 2.4–2.6 V for a blue/white LED) and thus starts conducting a reasonable amount of current. We also define this as "delay," the time passed after this instant. Measurements were carried out for currents ranging from 30 to 850 mA, with an arbitrary step of about 30 mA. After a pre-determined delay, the signals are averaged within a time window sufficiently narrow to avoid significant signal variations within each of them (the time positions of these windows are indicated by the dotted lines in Fig. 7). Results are illustrated in Fig. 8, where it is possible to observe the reconstructed $I-V$ and $L-I$ characteristics as functions of the delay after the turn-on time. It is clear that, especially at high currents, the operating voltage of the device decreases with increasing delay due to the bandgap narrowing caused by the self-heating [33], [34]. Similarly, a corresponding decrease in the optical power emission can also be observed at high current [35] due to the increase in the rate of loss processes (such as Shockley–Read–Hall recombination and carrier escape) at higher junction temperatures. This highlights the importance of carrying out pulsed characterization measurements in order to avoid the heating effect. Since most electrooptical properties of LEDs are strongly related to the $T_j$ of the LED chip, it is fundamental to perform isothermal measurements and accurately determine the $T_j$ value in order to have a correct interpretation of the device behavior [6].

## VI. Tj Estimation

To quantify the increase in $T_j$ during the self-heating transients, it is possible to extrapolate a relation between $T_j$ and the device voltage, at a given bias current [32], [36]. The procedure consists of repeating the transient measurements at different device temperatures (in our case, the mount temperature was controlled by a TEC). Assuming that before the self-heating procedure, the junction temperature is equal to the baseplate temperature, it is possible to derive the dependence of device voltage on junction temperature from the very first part of measured voltage transient. Fig. 9 shows the voltage transients of a white high-power commercial LED recorded at different temperatures at 1 A, and the inset reports the relation between $T_j$ and the device voltage extrapolated from the transients. The latter follows an exponential trend that can be fit with a good accuracy. Therefore, it is possible to plot the $T_j$ trend (dashed line) during heating transient at 25 °C,

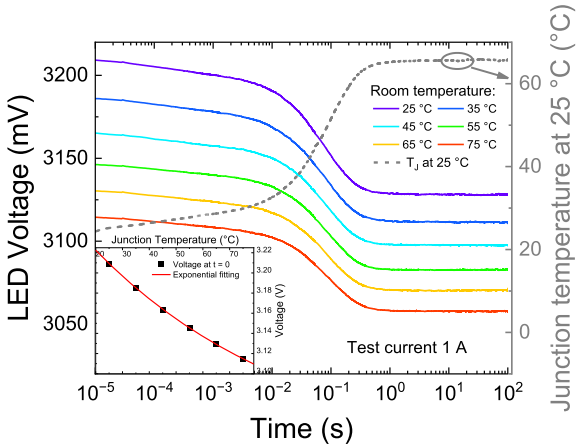


Fig. 9. Example of extrapolation of the relation between $T_j$ and the device voltage and the junction temperature trend of a commercial high-power white LED. The voltage transient measurement is repeated for different temperatures and the inset reports the junction temperature as function of the LED voltage. The black dashed line shows the junction temperature trend at a plate temperature of 25 °C, with a power dissipation around 1.9 W.

by converting the voltage values obtained from the analysis. In particular, the steady-state value of the LED voltage allows us to extract the $T_j$ after heating. It is interesting to observe an increase of about 40 °C in 1 s.

## VII. Spectral Measurements

Self-heating can also impact on the spectral characteristics of the devices. To evaluate this aspect, a first measurement of the power spectral densities of a high-power LED, emitting at about 630 nm, respectively, was carried out by an Ocean Optics USB4000 spectrometer. Measurements were carried out at different current levels, ranging from 50 mA to 1.05 A, and in two different conditions, dc and pulsed current. Pulsed measurements were performed with a pulsewidth of 30 $\mu$s and a period of 1 ms to keep a low duty cycle (3%) and minimize self-heating. The minimum integration time of the spectrometer was set to 30 ms to acquire a sufficient number of periods, thus ensuring adequate measurement uncertainty, since the obtained spectra is the average of all the acquisitions.

Fig. 10(a) shows the peak wavelength versus current relation of the spectra acquired by performing the measurements in continuous and pulsed condition. One can notice that for a red LED [Fig. 10(a)], a red shift of the emission prevails at increasing current. Additionally, this trend is more pronounced for the continuous measurement, leading to a 5.5 nm red shift: this is in line with expectations, since in the pulsed case, the lower self-heating strongly reduces the red-shift associated with the increase in junction temperature [37], that is a mere 0.5 nm. In Fig. 10(b), the full width at half maximum (FWHM) of the red spectra are compared under continuous and pulsed current. It can be noticed that there is a larger variation under continuous current (4 nm) than with pulsed measurement (2 nm).

Nevertheless, contrary to existing systems, this current source—coordinated with a fast spectrometer with external triggering—allows to perform spectral measurements during

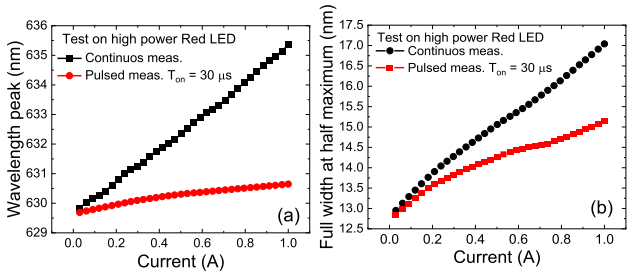


Fig. 10. In (a) comparison between the peak emission wavelength trends of the red LED under test as function of the current in continuous current (black) and pulsed current condition (red curves). In (b) comparison between the spectral width.

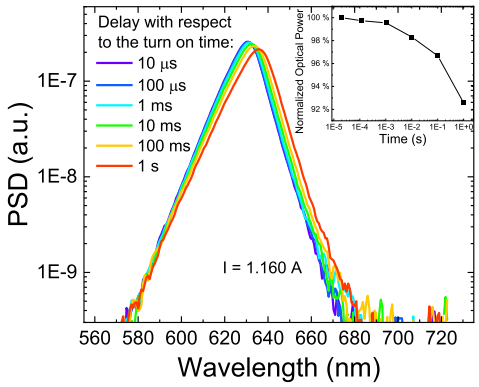


Fig. 11. Spectrum of a high-power red LED at exponentially spaced intervals during the heating transient in logarithmical scale. The inset represents the normalized optical power emission as function of the heating time.

the heating transient in a single acquisition. The fast spectrometer that we selected allows to perform the measurements with an integration time of 10 $\mu$s. Thus, the first spectrum available is only after a 20 $\mu$s current pulse, (10 $\mu$s for the settling time and the other 10 $\mu$s for the spectrum acquisition). By repeating the measurement at exponentially spaced intervals during the whole transient, it is possible to record the trend of the whole emission spectrum during the device self-heating. This provides useful information, such as the wavelength peak variation or the phosphors behavior, that would not be available with the only optical transients recorded by a photodetector.

We note here that such analysis requires a fast circuit and a fast spectrometer; a similar study could not be done by using a fast circuit and a photodiode. In fact, the gain function of commercial photodiodes is not flat, but varies as a function of the wavelength. This can lead to artifacts in the optical transient (such as increase in the emission due to variation in the wavelength peak during the heating). The characterization by means of spectral measurements overcomes these issues providing the correct trend. Thus, this system provides a fast-spectral characterization during a single heating transient. In Fig. 11, we report an example of spectrum acquisition during a heating transient of a high-power red LED.

## VIII. Conclusion

In this study, we presented a measurement system for the transient and pulsed characterization of power LEDs

and diodes that allow to measure the electrical, optical, and spectral performance of the devices by means of short (20 $\mu$s) current pulses in iso-thermal conditions. This is a significant advancement with respect to state-of-the-art LED qualification measurements, which mainly work either with pulses longer than 10–100 ms, or in dc conditions. In addition, the system allows to generate a constant current over several decades of time from 20 $\mu$s to 100 s and beyond, with good temporal stability (<0.1%). This is ideal for the characterization of the self-heating transients and the evaluation of LED thermal resistance. The proposed setup and approach have been validated through the characterization of commercially available LEDs. We presented the detailed results of the impact of the delay from the turn-on of the electrical and optical performance of the devices. The results highlight the importance of pulsed measurements for LED characterization, both in terms of spectral properties (such as peak wavelength, radiant power, linewidth) and of electrical parameters. Furthermore, it provides a powerful tool for a complete analysis of the heating transients of voltage and optical emission and the extrapolation of the structure function of the device [17], useful for reliability investigation [38] or for diagnostic aims [39] in the lighting industry. In fact, the study of the thermal impedance allows to identify the critical layers of the overall device structure, including the package [40]. The approach proposed within this article can be used to advance the state of the art on visible LED characterization, both at laboratory and industrial levels. With minor adaptations, it can also be exploited for other optoelectronic and microelectronics devices, such as UV LEDs [41], laser, and high-power diodes.

## Acknowledgment

The presented results are reflecting only the author's view: ECSEL-JU is not responsible for any use that may be made of the information it contains.

## References

[1] F. M. Steranka et al., "High power LEDs—Technology status and market applications," *physica status solidi*, vol. 194, no. 2, pp. 380–388, 2002, doi: 10.1002/1521-396X(200212)194:2<380:AID-PSSA380>3.0.CO;2-N.

[2] T. Kachi, "Recent progress of GaN power devices for automotive applications," *Jpn. J. Appl. Phys.*, vol. 53, no. 10, 2014, Art. no. 100210, doi: 10.7567/JJAP.53.100210.

[3] T. Miyoshi, T. Kozaki, T. Yanamoto, Y. Fujimura, S. Nagahama, and T. Mukai, "GaN-based high-output-power blue laser diodes for display applications," *J. Soc. Inf. Display*, vol. 15, no. 2, pp. 157–160, Feb. 2007, doi: 10.1889/1.2709737.

[4] J. Hu, L. Yang, and M. W. Shin, "Electrical, optical and thermal degradation of high power GaN/InGaN light-emitting diodes," *J. Phys. D, Appl. Phys.*, vol. 41, no. 3, Feb. 2008, Art. no. 035107, doi: 10.1088/0022-3727/41/3/035107.

[5] L. Yang, J. Hu, S. Jang, and M. W. Shin, "Thermal design of ceramic packages for high power light-emitting diodes," *Semicond. Sci. Technol.*, vol. 22, no. 7, pp. 705–708, Jul. 2007, doi: 10.1088/0268-1242/22/7/005.

[6] G. A. Onushkin et al., "Assessment of isothermal electro-optical-thermal measurement procedures for LEDs," in *Proc. 23rd Int. Workshop Thermal Investigations ICs Syst. (THERMINIC)*, Sep. 2017, pp. 1–6, doi: 10.1109/THERMINIC.2017.8233796.

[7] JEDEC. *Transient Dual Interface Test Method for the Measurement of the Thermal Resistance Junction-to-Case of Semiconductor Devices With Heat Flow Through a Single Path*. Accessed: Nov. 24, 2022. [Online]. Available: https://www.jedec.org/standards-documents/docs/jesd51-14-0

[8] C.-P. Wang, T.-T. Chen, H.-K. Fu, T.-L. Chang, and P.-T. Chou, "Transient analysis of partial thermal characteristics of multi-structure power LEDs," *IEEE Trans. Electron Devices*, vol. 60, no. 5, pp. 1668–1672, May 2013, doi: 10.1109/TED.2013.2252903. https://doi.org/10.1109/TED.2013.2252903.

[9] M. E. Raypah, M. Devarajan, A. A. Ahmed, and F. Sulaiman, "Thermal characterizations analysis of high-power ThinGaN cool-white light-emitting diodes," *J. Appl. Phys.*, vol. 123, no. 10, 2018, Art. no. 105703, doi: 10.1063/1.5016359.

[10] T. Dannerbauer and T. Zahner, "Inline rth control: Fast thermal transient evaluation for high power LEDs," in *Proc. 19th Int. Workshop Thermal Investigations ICs Syst. (THERMINIC)*, Sep. 2013, pp. 172–175, doi: 10.1109/THERMINIC.2013.6675208.

[11] C. Cengiz, M. Azarifar, and M. Arik, "A critical review on the junction temperature measurement of light emitting diodes," *Micromachines*, vol. 13, no. 10, p. 1615, Sep. 2022, doi: 10.3390/mi13101615.

[12] G. Hantos, J. Hegedüs, and A. Poppe, "Different questions of today's LED thermal testing procedures," in *Proc. 34th Thermal Meas., Model. Manage. Symp. (SEMI-THERM)*, Mar. 2018, pp. 63–70, doi: 10.1109/SEMI-THERM.2018.8357354.

[13] M. C. Bein et al., "Comparison of two alternative junction temperature setting methods aimed for thermal and optical testing of high power LEDs," in *Proc. 23rd Int. Workshop Thermal Investigations ICs Syst. (THERMINIC)*, Sep. 2017, pp. 1–4, doi: 10.1109/THERMINIC.2017.8233838.

[14] G. Farkas, M. C. Bein, and L. Gaál, "Multi domain modelling of power LEDs based on measured isothermal and transient I-V-L characteristics," in *Proc. 22nd Int. Workshop Thermal Investigations ICs Syst. (THERMINIC)*, Sep. 2016, pp. 181–186, doi: 10.1109/THERMINIC.2016.7749049.

[15] A. Poppe, G. Farkas, L. Gaál, G. Hantos, J. Hegedüs, and M. Rencz, "Multi-domain modelling of LEDs for supporting virtual prototyping of luminaires," *Energies*, vol. 12, no. 10, p. 1909, May 2019, doi: 10.3390/en12101909.

[16] L. Mitterhuber et al., "Investigation of the temperature-dependent heat path of an LED module by thermal simulation and design of experiments," in *Proc. 22nd Int. Workshop Thermal Investigations ICs Syst. (THERMINIC)*, Sep. 2016, pp. 194–200, doi: 10.1109/THERMINIC.2016.7749051.

[17] A. Alexeev, G. Onushkin, J.-P. Linnartz, and G. Martin, "Multiple heat source thermal modeling and transient analysis of LEDs," *Energies*, vol. 12, no. 10, p. 1860, May 2019, doi: 10.3390/en12101860.

[18] A. Noeman, "High-side current sources for industrial applications," *Analog Des. J.*, 2019. Accessed: Nov. 24, 2022. [Online]. Available: https://www.ti.com/lit/an/slyt768/slyt768.pdf

[19] C. Wells and D. F. Chan. (2013). *High-Side Voltage-to-Current (V-I) Converter*. Accessed: Nov. 24, 2022. [Online]. Available: https://www.ti.com

[20] T.-H. Liu, H.-T. Cheng, J.-Y. Wu, and C.-H. Wu, "Achieving ns-level pulsed operation of up to 6.27 W with a 1.55-$\mu$m BH-DFB laser for LiDAR applications," *Opt. Lett.*, vol. 48, no. 11, p. 3071, Jun. 2023, doi: 10.1364/ol.494220.

[21] H. Halbritter, C. Jäger, R. Weber, M. Schwind, and F. Möllmer, "High-speed LED driver for ns-pulse switching of high-current LEDs," *IEEE Photon. Technol. Lett.*, vol. 26, no. 18, pp. 1871–1873, Sep. 15, 2014, doi: 10.1109/LPT.2014.2336732.

[22] E. Abramov, M. Evzelman, O. Kirshenboim, T. Urkin, and M. M. Peretz, "Low voltage sub-nanosecond pulsed current driver IC for high-resolution LiDAR applications," in *Proc. IEEE Appl. Power Electron. Conf. Expo. (APEC)*, Mar. 2018, pp. 708–715, doi: 10.1109/APEC.2018.8341090.

[23] F. Henningsen, N. Braam, and M. Danninger, "Picosecond and high-power UV/Vis light pulsing using gallium nitride field-effect transistors: Implementation and design evaluation," *J. Instrum.*, vol. 18, no. 10, Oct. 2023, Art. no. P10010, doi: 10.1088/1748-0221/18/10/p10010.

[24] V. Székely and T. Van Bien, "Fine structure of heat flow path in semiconductor devices: A measurement and identification method," *Solid-State Electron.*, vol. 31, no. 9, pp. 1363–1368, Sep. 1988, doi: 10.1016/0038-1101(88)90099-8.

[25] M. van der Schans, J. Yu, and G. Martin, "Digital luminaire design using LED digital twins—Accuracy and reduced computation time: A Delphi4LED methodology," *Energies*, vol. 13, no. 18, p. 4979, Sep. 2020, doi: 10.3390/en13184979.

[26] L. Yang, J. Hu, and M. W. Shin, "Dynamic thermal analysis of high-power LEDs at pulse conditions," *IEEE Electron Device Lett.*, vol. 29, no. 8, pp. 863–866, Aug. 2008, doi: 10.1109/led.2008.2000953.

[27] Electronics Cooling. *Testing of Power LEDs: The Latest Thermal Testing Standards From JEDEC*. Accessed: Nov. 24, 2022. [Online]. Available: https://www.electronics-cooling.com/2013/09/testing-of-power-leds-the-latest-thermal-testing-standards-from-jedec/

[28] B. Pardo et al., "Thermal resistance investigations on new leadframe-based LED packages and boards," *Microelectron. Rel.*, vol. 53, no. 8, pp. 1084–1094, Aug. 2013, doi: 10.1016/j.microrel.2013.02.016.

[29] J. H. Choi and M. W. Shin, "Thermal investigation of LED lighting module," *Microelectron. Rel.*, vol. 52, no. 5, pp. 830–835, May 2012, doi: 10.1016/j.microrel.2011.04.009.

[30] L. Kim, J. H. Choi, S. H. Jang, and M. W. Shin, "Thermal analysis of LED array system with heat pipe," *Thermochimica Acta*, vol. 455, nos. 1–2, pp. 21–25, Apr. 2007, doi: 10.1016/j.tca.2006.11.031.

[31] E. Juntunen, O. Tapaninen, A. Sitomaniemi, and V. Heikkinen, "Effect of phosphor encapsulant on the thermal resistance of a high-power COB LED module," *IEEE Trans. Compon., Packag., Manuf. Technol.*, vol. 3, no. 7, pp. 1148–1154, Jul. 2013, doi: 10.1109/TCPMT.2013.2260796. https://doi.org/10.1109/TCPMT.2013.2260796.

[32] Y. Xi and E. F. Schubert, "Junction–temperature measurement in GaN ultraviolet light-emitting diodes using diode forward voltage method," *Appl. Phys. Lett.*, vol. 85, no. 12, pp. 2163–2165, Sep. 2004, doi: 10.1063/1.1795351.

[33] Y. P. Varshni, "Temperature dependence of the energy gap in semiconductors," *Physica*, vol. 34, no. 1, pp. 149–154, Jan. 1967, doi: 10.1016/0031-8914(67)90062-6.

[34] N. Sarkar and S. Ghosh, "Temperature dependent band gap shrinkage in GaN: Role of electron–phonon interaction," *Solid State Commun.*, vol. 149, nos. 31–32, pp. 1288–1291, Aug. 2009, doi: 10.1016/j.ssc.2009.05.008.

[35] A. Rashidi, M. Monavarian, A. Aragon, and D. Feezell, "Thermal and efficiency droop in InGaN/GaN light-emitting diodes: Decoupling multiphysics effects using temperature-dependent RF measurements," *Sci. Rep.*, vol. 9, no. 1, pp. 1–10, Dec. 2019, doi: 10.1038/s41598-019-56390-2.

[36] D. S. Meyaard, J. Cho, E. F. Schubert, S. H. Han, M. H. Kim, and C. Sone, "Analysis of the temperature dependence of the forward voltage characteristics of GaInN light-emitting diodes," *Appl. Phys. Lett.*, vol. 103, Sep. 2013, Art. no. 121103, doi: 10.1063/1.4821538.

[37] D. Peng and K. Jin, "The influence of driving current on emission spectra of GaN-based LED," in *Proc. Int. Conf. Electron. Optoelectronics*, vol. 2, Jul. 2011, pp. V2-148–V2-151, doi: 10.1109/ICEOE.2011.6013198.

[38] M. Cai et al., "A novel hybrid method for reliability prediction of high-power LED luminaires," in *Proc. 14th Int. Conf. Thermal, Mech. Multi-Physics Simulation Exp. Microelectron. Microsyst. (EuroSimE)*, Apr. 2013, pp. 1–5, doi: 10.1109/EuroSimE.2013.6529984.

[39] A. Hanß, M. Schmid, E. Liu, and G. Elger, "Transient thermal analysis as measurement method for IC package structural integrity," *Chin. Phys. B*, vol. 24, no. 6, Jun. 2015, Art. no. 068105, doi: 10.1088/1674-1056/24/6/068105.

[40] X. Lei et al., "Reduction of die-bonding interface thermal resistance for high-power LEDs through embedding packaging structure," *IEEE Trans. Power Electron.*, vol. 32, no. 7, pp. 5520–5526, Jul. 2017, doi: 10.1109/TPEL.2016.2609891. https://doi.org/10.1109/TPEL.2016.2609891.

[41] N. Trivellin et al., "On the importance of fast and accurate LED optical and thermal characterization: From visible use cases to UV technologies," in *Proc. 29th Int. Workshop Thermal Investigations ICs Syst. (THERMINIC)*, Sep. 2023, doi: 10.1109/therminic60375.2023.10325894.

Open Access funding provided by 'Università degli Studi di Padova' within the CRUI CARE Agreement